Tsunami Hazard Assessment of the Ocosta School Site in Westport, WA

Frank González, Randy LeVeque and Loyce Adams

University of Washington

Westport, WA, Google Earth image. Blue rectangle is area of fine resolution GeoClaw tsunami model grid; white circle encompasses Ocosta School campus;

Study funded by Washington State Emergency Management Division

1 Background

The probability that an earthquake of magnitude 8 or greater will occur on the Cascadia Subduction Zone (CSZ) in the next 50 years has been estimated to be 10-14% (Petersen, et al., 2002). The last such event occurred in 1700 (Satake, et al., 2003; Atwater, et al., 2005) and future events are expected to generate a destructive tsunami that will inundate Westport and other Washington Pacific coast communities within tens of minutes after the earthquake main shock.

A previous study by Walsh, et al. (2000) documented evidence of two tsunamis that struck the Southwest Washington Coast, generated in 1700 and 1964 by earthquakes on the Cascadia Subduction Zone (CSZ) and Alaska-Aleutian Subduction Zone (AASZ), respectively. Tsunami simulations were conducted for two magnitude 9.1 (M9.1) CSZ earthquake scenarios, one of which included an area of higher uplift and, therefore, a higher initial tsunami wave offshore of northern Washington. These simulations resulted in moderate to high inundation of Washington coastal communities, including Westport, WA.

The Westport Ocosta School District is now proposing the construction of a new building to replace the current Ocosta Elementary School (Educational Service District 112, 2012). Since the Walsh et al. (2000) study, there have been significant advances in tsunami modeling and our understanding of potential CSZ earthquake events. Consequently, this study was commissioned and funded by the Washington Emergency Management Division to meet the need for an updated assessment of the tsunami hazard at the Ocosta School campus.

2 Earthquake Scenarios

In the general context of tsunami hazard assessment and emergency management planning, there are two general classes of tsunamigenic earthquake scenarios that represent quite different threats. A *distant*, or *far-field*, earthquake generates a tsunami that must traverse the open ocean for hours, generally losing a significant percentage of the destructive energy it had in the generation zone. In dramatic contrast, a *local*, or *near-field*, earthquake generates a tsunami that arrives at a nearby community in tens of minutes with much smaller loss of energy during the short propagation distance from the generation zone. This study considers a tsunamigenic earthquake scenario of each type.

The *local* or *near*-field M9 earthquake on the CSZ simulated in this study is the L1 scenario developed by Witter, et al (2012); it is one of 15 seismic scenarios used in a hazard assessment study of Bandon, OR, based on an analysis of data spanning 10,000 years. There is significant uncertainty in assigning an average return period to the L1 scenario, but based on a simple analysis of the evidence presented by Witter et al. (2011) on the estimated ages of M9 and larger CSZ earthquakes, a range of 1990-3300 years seems reasonable (Witter, 2013). The L1 scenario was chosen as the near-field source for this study because the standard engineering planning horizon for this project is about 2500 years and, in the professional judgment of the authors, of all the events considered with magnitude greater than M9, L1 had the highest probability of occurrence. The length and width of L1 are approximately 1000 km and 85 km, respectively; salient features of the earthquake crustal deformation include subsidence at Westport of about 1-2 m and a zone of about 8 to 10 m maximum uplift about 75 km offshore of Westport (Figure 1).

The distant or far-field M9.2 earthquake on the AASZ simulated for this study is similar to the 1964 Alaska event, which was the second largest worldwide since about 1900, when earthquake recordings began. The associated tsunami caused tremendous loss of life and property in Alaska and Crescent City, CA. This same scenario was developed and used in a previous study of Seaside, OR (Gonzalez, et al., 2009) and was also included in the Witter, et al. (2012) study of Bandon, OR. The Tsunami Pilot Study Working Group (TPSWG, 2006) estimated the mean return period of this scenario to be about 750 years.

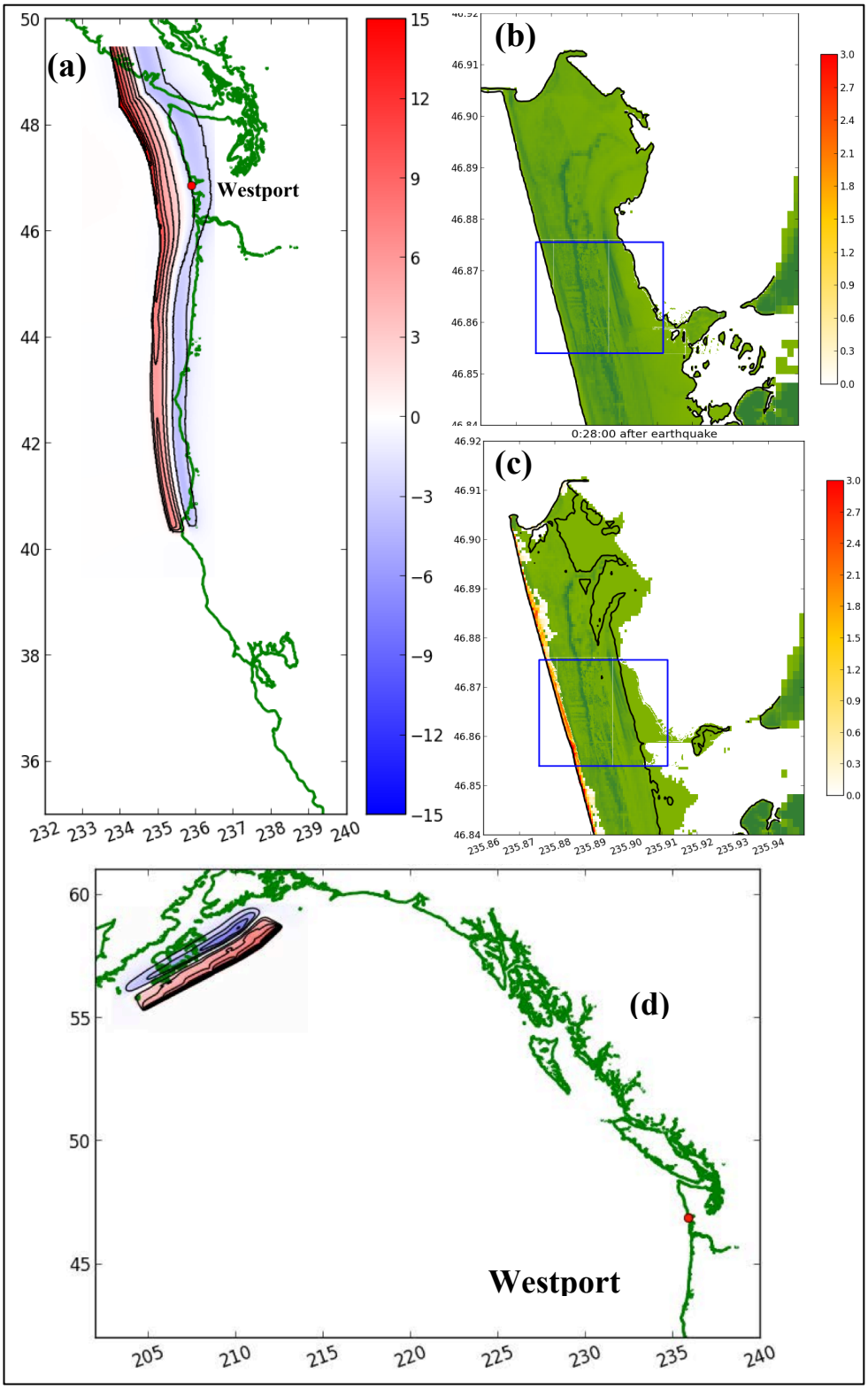

Figure 1. (a) CSZ earthquake vertical displacement, and initial tsunami waveform, in meters; note the coastal subsidence of 1-2 m at Westport. (b) Black line is Westport mean high water (MHW) before CSZ event. (c) Black line is Westport MHW after subsidence. The blue rectangles are 7-10 m resolution computational grid areas that encompass the Ocosta school site. (d) AASZ earthquake vertical displacement, with vertical scale as in (a).

3 Tsunami Modeling Results

The simulations of tsunami generation, propagation and inundation were conducted with the GeoClaw model. The GeoClaw model solves the nonlinear shallow water equations, has undergone extensive verification and validation (LeVeque and George, 2007; LeVeque, et al., 2011) and has been accepted as a validated model by the U.S. National Tsunami Hazard Mitigation Program (NTHMP) after conducting multiple benchmark tests as part of an NTHMP benchmarking workshop (NTHMP, 2012).

Computations of tsunami flooding on the Ocosta School campus and surrounding area (the blue rectangle in Figure 1b) were made on a fine resolution computational grid of 1/3 arc-second; at the mean latitude of the study site, this corresponds to linear dimensions of approximately 7m x 10m in the East-West and North-South directions, respectively. All simulations were conducted with the tide level set to Mean High Water (MHW), which is standard practice for studies of this type.

In the following sections we will compare and contrast important features of the CSZ and AASZ scenarios described above, in terms of the tsunami hazard posed to Westport in general and to the Ocosta School site, in particular. Section 5 then discusses some inherent uncertainties in the specification of the earthquake scenarios, the limitations of the GeoClaw model, and the associated uncertainties in the results.

3.1 Local Subsidence

Typically, subduction zone earthquakes are characterized by offshore uplift that generates the crest of an initial tsunami wave, nearshore subsidence that generates an initial tsunami wave trough offshore and coastal subsidence that can increase the depth of subsequent flooding on land. The initial wave splits in two; one wave propagates into the open ocean, the other propagates toward a coastal region that has now subsided and is therefore more susceptible to flooding. In the specific CSZ scenario modeled here, L1, the Westport peninsula is subjected to subsidence of about 1 – 2 m (Figures 1a-1c). The AASZ earthquake is too far away to induce subsidence on the Washington coast, although subsidence does occur on the local Alaskan coastline (Figure 1d).

3.2 Maximum Flood Depth

Figure 2 was obtained by storing the maximum computed flood depth (i.e., the depth of water above the local ground level) computed in each grid cell during the entire tsunami simulation. In both scenarios, flooding from Grays Harbor stops short of the Ocosta School buildings; relatively high N-S ridges to the east act as barriers that protect the Ocosta School campus from the tsunami waves that inundate the Pacific coast.

As expected, the areal extent and depth of flooding are much greater in the CSZ scenario than in the AASZ scenario. The AASZ scenario produces much less flooding that is restricted to a narrow strip of the beach, with essentially no flooding of the residential areas to the east.

In contrast, the CSZ scenario creates flooding in excess of 12 m extending eastward from the Pacific coast, through residential and downtown Westport, then across a system of north-south trending ridges to continue flooding eastward at a level of 5-10 m until reaching Montesano Street, located on a N-S ridge; this ridge is approximately 10 m above MHW, and protects the Ocosta School campus from the eastward flooding (Figure 3, Transects A and B). Note that some overtopping of the westernmost ridge does occur farther south, where the elevation of the ridge drops to about 7 m (Figure 2 and Figure 3, transect C).

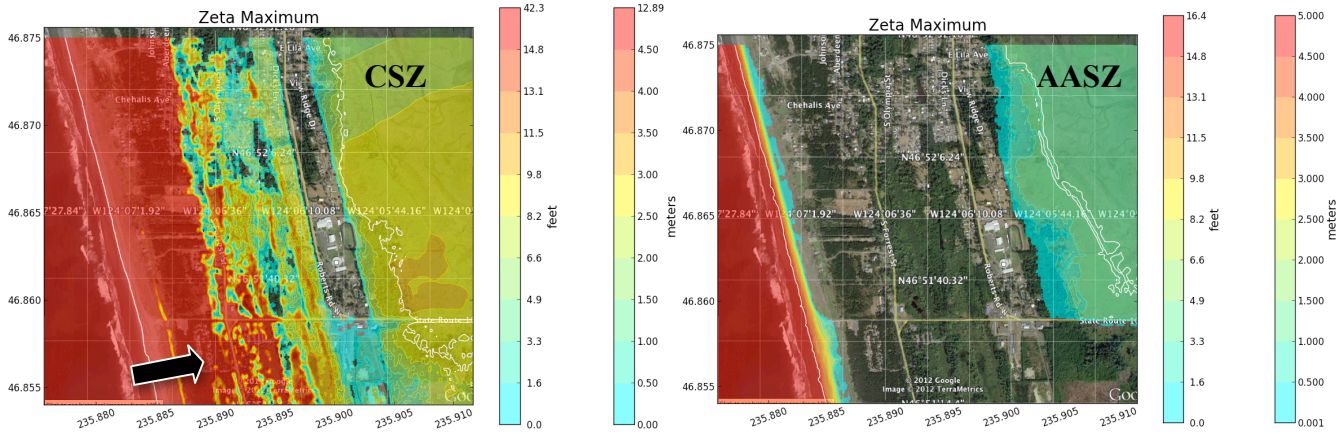

Figure 2. Maximum tsunami flooding depth for CSZ (left) and AASZ (right) event. Note the maximum depths at the top of the vertical color scales: 12.89 m (42.3 ft) for the CSZ event and 5.0 m (16.4 ft) for the AASZ event. The spatial resolution of the computational grid is1/3 arc-sec, or 7-10 m. The white lines are the coastline at MHW and the black arrow in the CSZ scenario (left panel) points to a relatively low area of the ridge that facilitates flooding to the east. Compare the new MHW coastline created by subsidence in the CSZ scenario (left), with the original coastline, which does not subside in the AASZ scenario (right).

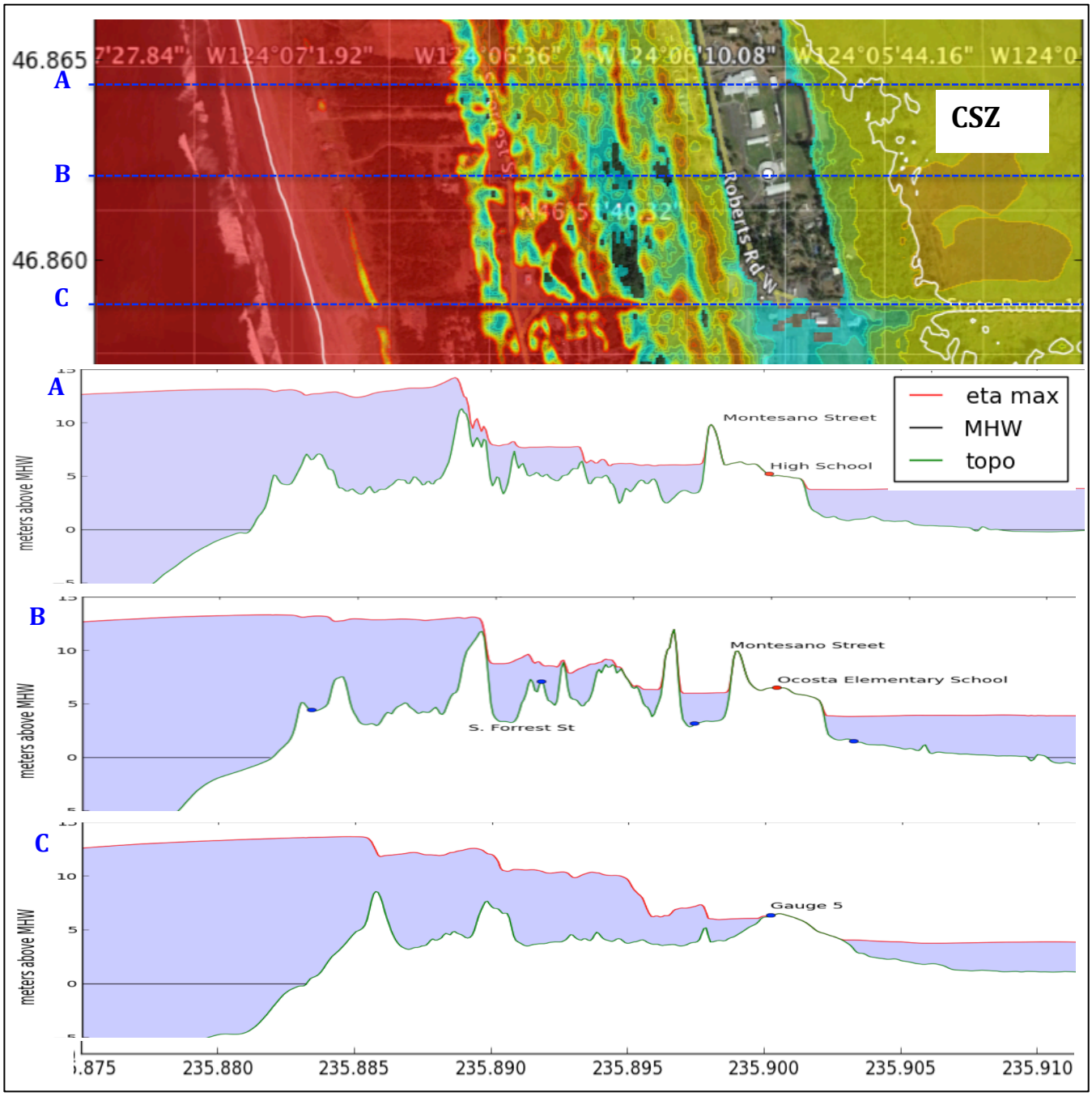

Figure 3. Top panel presents a section of the CSZ flooding graphic of Figure 2 and the location of E-W transects A, B and C through the High School, Elementary School and GeoClaw model Gauge 5 (located on State Route 105). Blue dots mark the location of GeoClaw model stations where tsunami time series were obtained.

3.3 Maximum Current Speed

Strong currents can be highly dangerous, demolishing structures and transporting logs, boats, automobiles and other rolling stock to form fields of debris that act as battering rams to multiply the destructive impact of the tsunami. Figure 4 presents the maximum current speed for both scenarios. The spatial pattern seen for maximum flood depth in Figure 2 is repeated, and the CSZ event produces extremely high speeds, with large areas characterized by values of 8-12 m/s; values are lower, 0.5-2 m/s, during the AASZ event.

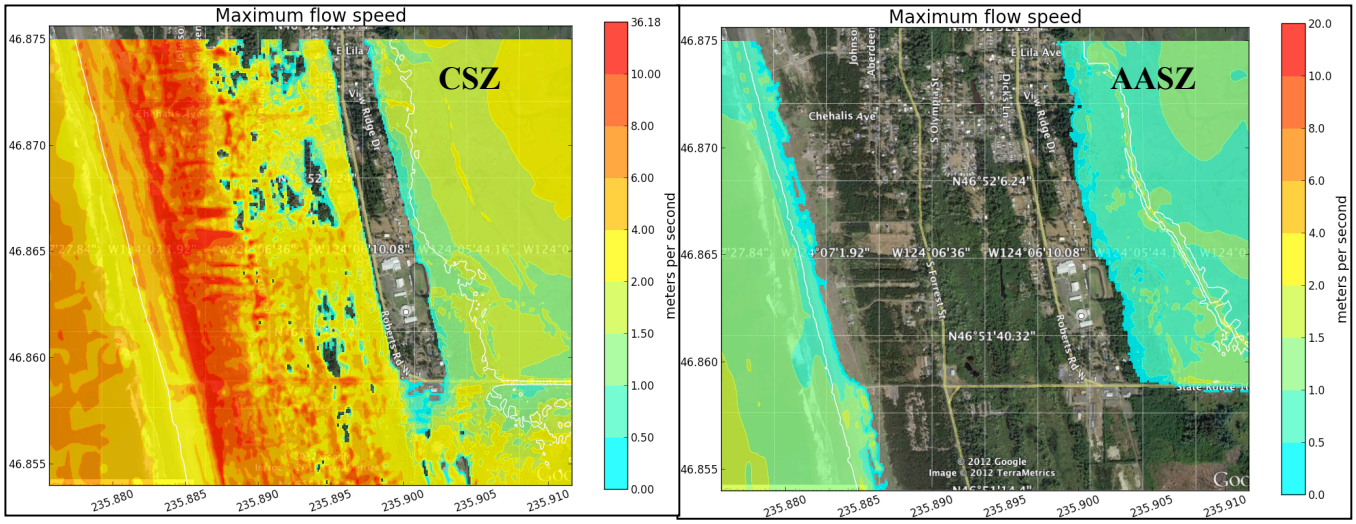

Figure 4. Maximum tsunami current speed for CSZ (left) and AASZ (right) earthquakes. Note the difference in scales: 0 - 36.18 m/s for the CSZ event and 0 - 20 m/s for the AASZ event (1 m/s = 2.2 mi/hr = 1.9 knots).

3.4 Arrival Time

Figure 5 presents the tsunami arrival times, referred to the time of the earthquake main shock, for each scenario. It takes the tsunami about 3.7 hours to traverse the Pacific from the AASZ off Alaska to

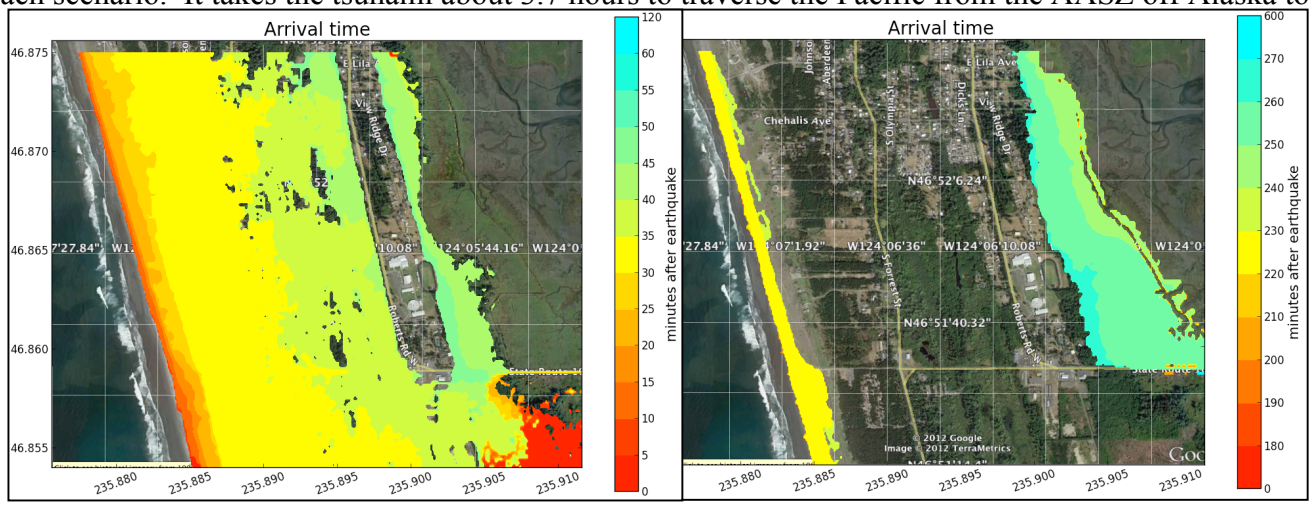

Figure 5. Tsunami arrival time after the main shock of an earthquake on the CSZ (left) and the AASZ (right). Note the difference in time scales – the maxima are 2 and 6 hours for the CSZ and AASZ events, respectively.

the Westport peninsula, while the tsunami generated in the CSZ strikes the Westport beach in less than 5minutes and engulfs much of the downtown and residential areas in less than 40 minutes; on the Gray's

Harbor side, the wave strikes the beach east of the Ocosta School campus in about 35 minutes and reaches the maximum inland extent in less than 50 minutes.

4 Uncertainties and Limitations

Numerical models do not produce perfect simulations of any natural process. Here we discuss uncertainties and limitations most important to this specific study and, where possible, their probable influence on the model output.

4.1 Source Specification

This is likely the largest source of uncertainty in the study. Variations in the value of certain earthquake parameters can produce large differences in the subsequent tsunami flooding.

Earthquake Magnitude and Recurrence Interval

In general, the greater the earthquake magnitude, the larger the initial wave amplitude (but see the discussion of slip distribution uncertainty, below, for exceptions to this general rule). With regards to the CSZ event, however, larger events would be associated with larger recurrence intervals than the estimated 1990-3300 years (Witter, 2013) and would be longer than the standard 2500 year planning horizon. In addition, Witter et al. (2011) estimate that "…the L1 scenario captures 95 percent of the hazard and more severe events are extremely unlikely."

The AASZ event is similar to a historic event, the 1964 Prince William Sound earthquake, and the magnitude was estimated from direct measurements. Such events are estimated to occur more frequently than great CSZ events, with a recurrence interval of about 750 years (TPSWG, 2006), but the threat to the Ocosta School campus from such great earthquakes is greatly mitigated by the large distance the tsunami must traverse to the site.

Earthquake Slip Distribution

The vertical displacement of the earth's crust presented in Figure 1 (a) is the direct result of a Pacific oceanic tectonic plate slipping (or subducting) beneath the North American continental plate, deforming both plates in the process. But the amount of slip is not distributed evenly on the common surface, known as the fault plane, where the two plates are in direct contact. There are patches on the fault plane, known as asperities, in which the two plates are more tightly locked by friction or protrusions of one plate into the other. But the relentless movement of the tectonic plates over decades and centuries continues to build up stress until the rock in the asperity region breaks and the plates slip past one another.

Most earthquake energy is released by the slip in asperities, and the larger the slip, the greater the earthquake energy. As a consequence, details of the slip distribution can make a significant difference in the initial amplitude of a tsunami; for example, if the slip is distributed evenly over the entire fault plane, then the initial tsunami amplitude will be about half the amplitude of a tsunami generated by slip distributed evenly over half of the fault plane. In particular, high slip values concentrated in an asperity region are associated with large values of vertical displacement of the ocean floor and a higher initial tsunami wave in the region.

Thus, the location of a coastal community relative to an asperity and the associated high wave region can have a direct effect on the severity of flooding in the community. When an earthquake is in the far-field, such as the AASZ scenario considered here, the earthquake resembles a point or line source and the details of the slip distribution are not important. However, details of the near-field slip distribution for the CSZ scenario L1 can affect Westport inundation. For example, about 75 km northwest of Westport there is an offshore maxima of 10-12 m in crustal deformation and the initial tsunami waveform (Figure 1(a)); if this maxima was located farther or closer to Westport, the inundation would

likely increase or decrease, respectively. Similarly, if the concentration of slip (and therefore earthquake energy) resulted in a larger or smaller maximum value, then a corresponding increase or decrease in flooding would be expected. However, it is not possible to make a reliable prediction of slip distribution at this level of detail, and conducting numerical experiments to estimate the sensitivity of flooding to such changes is beyond the scope of this study.

Landslide sources

This study did not include modeling of local landslides that are triggered by earthquake shaking. The impact of tsunamis generated by landslides is restricted to the local generation area, so that this is not an important process in the case of a far-field event like the AASZ earthquake used in this study. However, submarine landslides offshore the Pacific and Grays Harbor coasts of Westport could increase the severity of flooding.

4.2 Model Physics

Certain values were assumed for important geophysical parameters, and some physical processes were not included in the simulations; their potential effect on the modeling results are discussed below.

Tide Stage

The simulations were conducted with the background sea level set to MHW. This value is conservative, in the sense that more severe inundation results if sea level had been set to a lower value. Larger tide levels do occasionally occur, but the assumption of MHW is standard practice in studies of this type.

Friction

Manning's coefficient of friction was set to 0.025, a standard value used in tsunami modeling that corresponds to gravelly earth. This choice of 0.025 is conservative, because the presence of trees and vegetation to the west and east of the Ocosta campus would justify the use of a larger value, which would have the effect of reducing inundation.

Structures

Buildings were not included in the simulations. The presence of structures will alter tsunami flow patterns and generally impede inland flow. The lack of structures in the model is therefore a conservative feature, in that their inclusion would generally reduce inland penetration of the tsunami wave.

Debris

Large tsunamis inevitably create fields of debris that act as battering rams, multiplying the destructive impact. This process requires the expenditure of tsunami energy, which would tend to reduce the inland extent of the inundation.

Tsunami modification of bathymetry and topography

Severe scouring and deposition are known to occur during a tsunami, undermining structures and altering the flow pattern of the tsunami itself. Again, this movement of material requires an expenditure of tsunami energy that tends to reduce the inland extent of inundation and thereby reduce the risk to the Ocosta campus. However, it must be noted that erosion of the ridge west of campus could greatly increase flooding.

5 Discussion

Numerical simulations of Westport tsunami inundation resulting from two scenarios – a near-field CSZ earthquake and a far-field AASZ earthquake scenario produced no flooding of the Ocosta School campus, although severe flooding was inflicted on the Pacific coast and much of downtown and

residential Westport by the near-field CSZ event. The primary source of uncertainty in these results is in the specification of the CSZ earthquake characteristics, especially the details of the seismic slip distribution. Since numerical experiments were not conducted to estimate the sensitivity of Ocosta campus flooding to these source uncertainties, it is impossible to rule out a future earthquake with a slip distribution that would increase flooding near the Ocosta school campus, although it seems likely that the resulting increase caused by such an event would only be a modest fraction of the flooding simulated in this study. The effect of values chosen for the background sea level and Mannings coefficient of friction is a tendency to overestimate the severity of flooding. But physical processes such as wave/structure interaction, debris flow, scouring and deposition, were not included in the model, and these could increase flooding. Because of the above uncertainties, the results must be used with caution.

References

Atwater, Brian F, Musumi-Rokkaku Satoko, Kenji Satake, Tsuji Yoshinobu, Ueda Kazue, and David K Yamaguchi (2005): USGS Professional Paper 1707, pp 1–144.

Educational Service District 112 (2012): Facility Master Plan for the Ocosta School District, 68 pp, including 4 Appendices. (Available at http://www.ocosta.k12.wa.us/pages/Ocosta_School_District__172/Elementary_School_Bond)

Gonzalez, F I, E L Geist, B Jaffe, U Kânoğlu, H Mofjeld, C E Synolakis, V V Titov, et al. (2009): Probabilistic Tsunami Hazard Assessment at Seaside, Oregon, for Near- and Far-Field Seismic Sources, *Journal of Geophysical Research* 114 (C11) (November 24). doi:10.1029/2008JC005132.

LeVeque, J and D. L. George (2007): High-resolution finite volume methods for the shallow water equations with bathymetry and dry states. In P. L-F. Liu, H. Yeh, and C. Synolakis, editors, Advanced Numerical Models for Simulating Tsunami Waves and Runup, volume 10, pp 43-73. http://www.amath.washington.edu/ rjl/pubs/catalina04/.

LeVeque, R. J., D. L. George, and M. J. Berger (2011): Tsunami modeling with adaptively refined finite volume methods. Acta Numerica, pp 211-289.

NTHMP (National Tsunami Hazard Mitigation Program) (2012): Proceedings and Results of the 2011 NTHMP Model Benchmarking Workshop. Boulder: U.S. Department of Commerce/NOAA/NTHMP (NOAA Special Report) 436 pp.

Petersen, M. D., C. H. Cramer, and A. D. Frankel (2002): Simulations of Seismic Hazard for the Pacific Northwest of the United States from Earthquakes Associated with the Cascadia Subduction Zone. Pure Appl. Geophys., 159, 2147-2168.

Plafker, George, K.R. Lajoie, and Meyer Rubin (1992): Determining recurrence intervals of great subduction zone earthquakes in southern Alaska by radiocarbon dating: in Taylor, R.E., Long, Austin, and Kra, R.S., eds., Radiocarbon After Four Decades: An Interdisciplinary Perspective, New York, Springer-Verlag, pp. 436-453.

Satake, Kenji, Kelin Wang and Brian F Atwater (2003): Fault Slip and Seismic Moment of the 1700 Cascadia Earthquake Inferred From Japanese Tsunami Descriptions, *Journal of Geophysical Research* 108 (B11): 1–17. doi:10.1029/2003JB002521.

TPSWG (2006): Seaside, Oregon Tsunami Pilot Study— Modernization of FEMA Flood Hazard Maps." *Joint NOAA/USGS/FEMA Report* (November 2): 1–176.

Walsh, T. J., C.G. Caruthers, A.C. Heinitz, E.P. Myers, III, A.M. Baptista, G.B. Erdakos, R.A. Kamphaus (2000): Tsunami hazard map of the southern Washington coast: Modeled tsunami inundation from a Cascadia Subduction Zone earthquake. Washington Division of Geology and Earth Resources Geologic Map GM-49, 1 sheet, scale 1:100,000, with 12 p. text.

Witter, Robert C, Yinglong Zhang, Kelin Wang, George R Priest, Chris Goldfinger, Laura L Stimely, John T English, and Paul A Ferro (2011): Simulating Tsunami Inundation at Bandon, Coos County, Oregon, Using Hypothetical Cascadia and Alaska Earthquake Scenarios. *DOGAMI Special Paper 43* (July 11): 1–63.

Witter, Robert C. (2013): Personal Communication.